Journal of Marine Science and Engineering

MDPI

Article

Rhodolith Beds Heterogeneity along the Apulian Continental Shelf (Mediterranean Sea)

Giovanni Chimienti [1,2,*], Lucia Rizzo [2,3], Sara Kaleb [4], Annalisa Falace [4], Simonetta Fraschetti [2,3,5], Francesco De Giosa [6], Angelo Tursi [1,2], Enrico Barbone [7], Nicola Ungaro [7] and Francesco Mastrototaro [1,2]

[1] Department of Biology, University of Bari Aldo Moro, Via Orabona 4, 70125 Bari, Italy; angelo.tursi@uniba.it (A.T.); francesco.mastrototaro@uniba.it (F.M.)
[2] CoNISMa, Piazzale Flaminio 9, 00196 Roma, Italy; lucia.rizzo@szn.it (L.R.); simonetta.fraschetti@unina.it (S.F.)
[3] Stazione Zoologica Anton Dohrn, Villa Comunale, 80122 Napoli, Italy
[4] Department of Life Sciences, University of Trieste, Via Giorgieri 10, 34127 Trieste, Italy; sara.kaleb@gmail.com (S.K.); falace@units.it (A.F.)
[5] Department of Biology, University of Naples Federico II, Via Vicinale Cupa Cintia 21, 80126 Napoli, Italy
[6] Environmental Surveys S.r.l. (ENSU), Via De Gasperi, 74123 Taranto, Italy; francescodegiosa@ensu.it
[7] Apulian Regional Agency for the Environmental Prevention and Protection, Corso Trieste 27, 70126 Bari, Italy; e.barbone@arpa.puglia.it (E.B.); n.ungaro@arpa.puglia.it (N.U.)
* Correspondence: giovanni.chimienti@uniba.it; Tel.: +39-080-544-3330

Received: 25 September 2020; Accepted: 17 October 2020; Published: 19 October 2020

Abstract: Rhodolith beds represent a key habitat worldwide, from tropical to polar ecosystems. Despite this habitat is considered a hotspot of biodiversity, providing a suite of ecosystem goods and services, still scarce quantitative information is available thus far about rhodolith beds occurrence and ecological role, especially in the Mediterranean Sea. This study reports the composition and patterns of distribution of rhodolith assemblages found in four study areas along ca. 860 km of coast in the Central Mediterranean Sea. These rhodolith beds were studied for the first time and significant differences at all spatial scales have been highlighted, documenting the high variability of this habitat. Rhodolith species composition, morphology and distribution have been discussed considering the potential role of environmental factors in driving these patterns. The need for improving their protection is discussed to complement present conservation and management initiatives, particularly in the frame of the EU Marine Strategy Framework Directive.

Keywords: rhodolith bed; maërl; coralline algae; rhodophyta; habitat mapping; biogenic habitats; conservation; Marine Strategy; Mediterranean Sea

1. Introduction

Human activities largely affect natural systems, but their cumulative effects on ecological communities remains largely unknown [1]. A low diversity of species can affect ecosystems sensitivity to multiple stressors and enhance the impacts on ecosystem functioning [2]. For this reason, understanding patterns of distribution of species, communities and habitats is a priority to tease apart natural patterns from those driven by human disturbances [3]. Biodiversity in marine ecosystems is related to habitat heterogeneity [4], which is enhanced by ecosystem engineers, i.e., organisms that modify, maintain or destroy habitats [5–7]. Rhodolith-forming algae grow as unattached nodules, often acting as ecosystem engineers and forming aggregations known as Rhodolith Beds (RBs) on flat or gently-sloped seabed [5,6,8]. RBs provide habitat for several associated species from the tropics to polar latitudes [6,9–12], as well as a suite of ecosystem goods

and services whose economic importance encompasses biodiversity and fishery resources, soil conditioning and building industry, carbon trapping and climate regulation [13–20].

Rhodoliths three-dimensional complexity has been classified in three major categories along a continuum: compact and nodular pralines, large and vacuolar boxworks, and unattached branches [17]. RBs can be monospecific or they can be composed by a pool of species with different morphologies [21,22]. The current state of knowledge about Mediterranean RBs is overall fragmented and incomplete, with limited information about distribution, habitat structure, algal species composition and vitality [15,17,23–26].

An increased attention towards the status of RBs has been recently developed within the EU Marine Strategy Framework Directive (MSFD) [27] aiming to identify the Good Environmental Status (GES) [28]. The need for protection of this particular habitat and its algal bioconstructors has been also pointed out also in the EU Habitat Directive [29], the Bern Convention [30] and the Council Regulation 1967/2006 [31]. Moreover, Mediterranean RBs are subject of a special plan for protection within the framework of the United Nations Programme's Mediterranean Action Plan [32], although it is not mandatory for the national governments. Italy is among the European Countries that adopted these regulations and, in the last five years, a regional-scale systematic monitoring program is ongoing in order to cope with the substantial lack of knowledge about RBs distribution, ecology and functional role. In this framework, the possibility of adopting a specific experimental design for studying Mediterranean RBs has been suggested [17], since other approaches have been developed and calibrated on less heterogeneous Atlantic RBs, at shallower depth [33–35]. In fact, Mediterranean RBs are characterized by a remarkable diversity of coralline algae species and morphologies, often with more heterogeneous assemblages than the Atlantic ones [22,25,36,37], although an unexpected diversity in the northeast Atlantic RBs has been recently revealed by DNA barcoding [38].

The aim of this study is to assess the composition and pattern of distribution of RBs identified and monitored according to the MSFD in three out of four different areas of Apulia Region (Italy, Adriatic and Ionian Seas). The existence of relevant scales of variation across benthic habitats, on both hard and soft bottoms, has been documented in the last two decades [39–43]. Here, we use a hierarchical sampling design to examine spatial patterns in rhodolith assemblages at different scales (i.e., from meters to hundreds of kilometres) with a focus on rhodolith cover, taxonomic composition, morphologies and proportion of living thalli. We discuss the critical importance of new areas to be protected for the understanding of the status of this habitat in absence of evident sources of threats.

2. Materials and Methods

According to the definition of Steneck [44], we refer to rhodoliths as those free-living structures composed mostly (>50%) of calcareous red algae. More specifically, rhodoliths include pralines, boxwork and unattached branches morphotypes (this latter forming the so-called maërl) [6,17]. However, all the nodules showing a complete algal coating are considered as rhodolith for monitoring purposes, with no need to cut them [17]. We consider as RBs those sedimentary bottoms characterized by any morphology and species of unattached non-geniculate calcareous red algae (coated grains excluded) with >10% cover of living rhodoliths and a minimum extent of 500 m^2 [6,17]. On the basis of this definition, RBs include also maërl and fully calcified peyssonneliacean algae [10,45].

2.1. Study Areas

Four different areas of 25 km^2 each were surveyed along 865 km of coasts in the Apulia Region (Italy, Adriatic and Ionian Seas), from 10 to 62 m depth (Figure 1a–d). The Apulian continental shelf is characterized by coralligenous bioconstructions, such as a typical Mediterranean habitat built up by a suite of calcifying organisms (e.g., calcareous algae, corals, serpulids, bryozoans, molluscs) that grow one on the other, generation after generation, building a secondary hard substratum in dim light conditions [7,46–48]. The area is also characterized by a discontinuous belt of coastal detritic habitat (*sensu* [49]) that can coexist with, or bathymetrically follow, the coralligenous formations. Coastal detritic habitat can be dominated by rhodolith-forming algae that constitute RBs under

proper oceanographic and edaphic conditions [49]. However, records of RBs along the Apulian coast are old and uncertain [50–53], and no information about rhodoliths species composition, cover percentage, structure and main features is available.

The four study areas have been chosen according to the above-mentioned old records, considering the poor predictability of RB occurrence [54], and investigated from 2015 to 2017. These areas are located at Tremiti Islands Marine Protected Area (MPA; 42°07′ N, 15°30′ E; surveyed during October 2017; Figure 1a), northwest Otranto (40.14° N, 18.28° E; surveyed during November 2015; Figure 1b), off Gallipoli (40.07° N, 17.53° E; surveyed during June 2015; Figure 1c) and at Armeleia shoal (Taranto Gulf; 40.20° N, 17.06° E; surveyed during November 2016; Figure 1d). In particular, Tremiti Archipelago is located 12 nautical miles north of the Gargano promontory (Adriatic Sea) and is characterized by cold, oxygenated and trophic-carrying water masses, coming from the north and proceeding southwards, that support rich marine communities including extensive coral forests on coralligenous bioconstructions [55–57]. The MPA shows a gradient of restrictions and is divided into three main zones: Zone A (no take, no entry zone), Zone B (highly protected zone; anchoring and recreational fishing are forbidden, while professional fishing is regulated), and Zone C (partially protected zone; all human activities are allowed and professional fishing is regulated). The area northwest Otranto is located in proximity of the Otranto Strait (Adriatic Sea), where the scarp that bounds the Salento Peninsula slopes eastward down to the sea and dips at relatively high angle down to about 50 m depth [53]. Patchy marine bioconstructions, mostly coralligenous, are present down to 100 m depth [58]. Off Gallipoli (Ionian Sea) the shelf break begins at ca. 120 m depth and is anticipated by three terraced surfaces located at 25–30, 50–60 and 110–120 m depth [59]. The seabed is characterized by coralligenous outcrops interspersed with coastal detritic and muddy bottoms [50,53]. Proceeding westwards in the Gulf of Taranto, the Armeleia shoal is characterized by a slope of rocks and coralligenous bioconstructions from 10 to 40 m depth. At the base of the shoal, large coralligenous outcrops are patchy present on a detritic bottom.

The mean surface circulation in the study areas is induced by north-coming cold winds in the Adriatic Sea, by fresh water input from the Po River in the northern sector, and by differences in water density between the Ionian and the Adriatic seas in the southern sector [53,60]. These surficial currents are active down to about 150 m depth [57,61] and consist of an elongated basin-wide cyclonic gyre, with southward currents near the Italian coasts [62,63], and sub-basin cyclonic-gyre cells [60]. In particular, they run along-shore north of the Gargano Promontory [64], leave the coast south of the same promontory and re-approach the coast parallel to the Murge Plateau near Bari [65], contour the Salento Peninsula and enter the Ionian Sea inducing an along-shore cyclonic gyre in the Taranto Gulf of a broadly lower intensity [66].

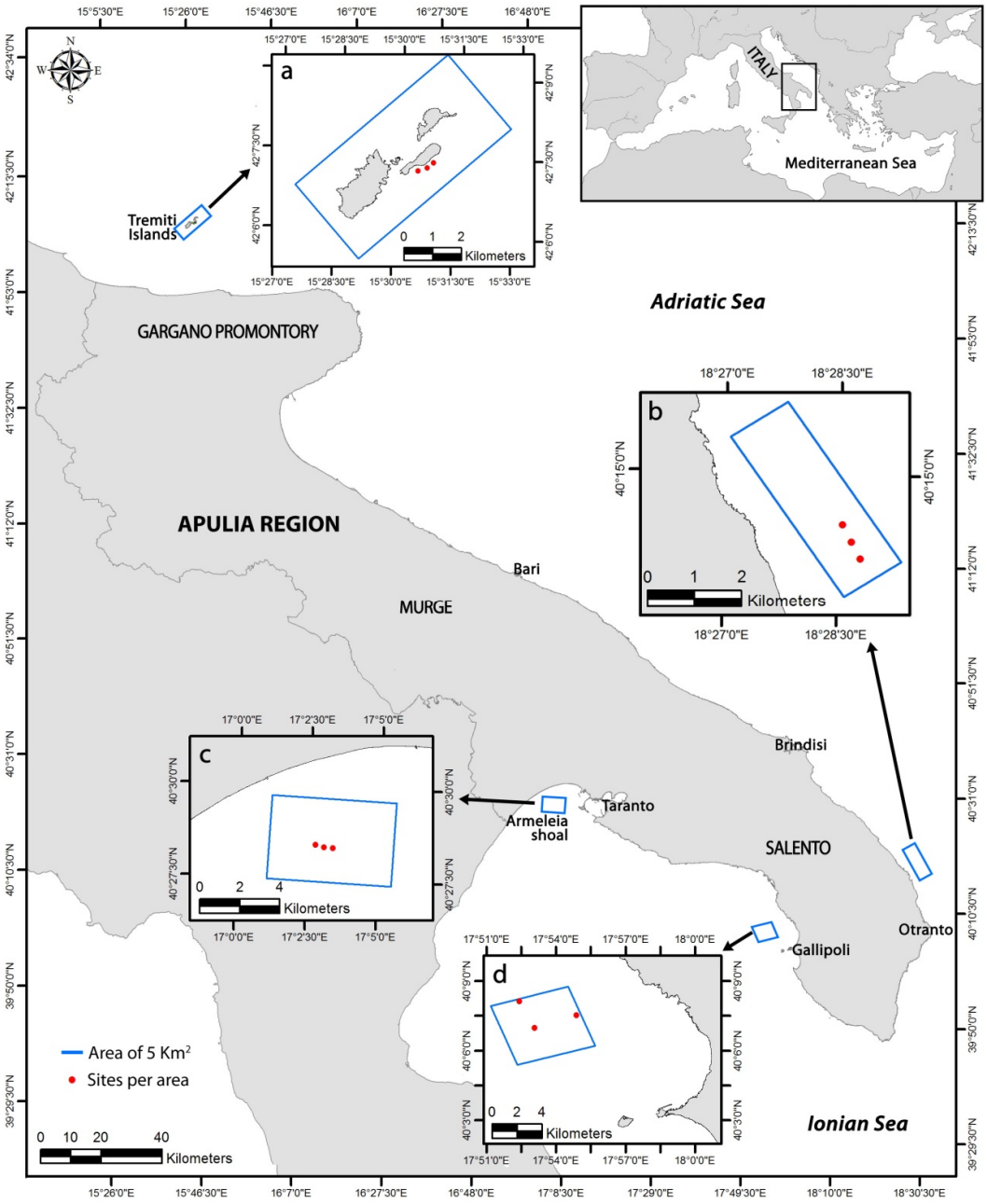

Figure 1. Map of Apulia Region. The four study areas are in blue: (**a**) Tremiti Islands Marine Protected Area (MPA); (**b**) northwest Otranto; (**c**) Armeleia shoal; (**d**) off Gallipoli. For each study area, three study sites (red dots) were selected for visual surveys and sampling.

2.2. *Habitat Mapping*

Mapping of the four study areas was carried out using Side-Scan Sonar (SSS; Klein 3000 and K3900) and MultiBeam EchoSounder (MBES; R2Sonic 2022 and RESON Seabat 8125) [8,17,32,67], for a total of 100 km² mapped.

SSS data were acquired with a double frequency of 100 and 500 kHz, simultaneously, using a swath width of 100 m, with 50% of overlap between adjacent lines. SSS data were processed using the CARIS HIPS and SIPS software, according to the following steps: data conversion; navigation processing; slant range correction; time varying gain application; attitude data editing; data mosaicing; data output. Geo-referenced, grey-tone acoustic images of the seafloor with a 0.2 m cell resolution were produced.

MBES data were acquired with the echo sounder mounted on a side pole solidly installed on vessel side. A SV probe was installed close to MBES transducer and connected to the system in order to measure sound speed in salt water to a real time correction of every acquired sounding. MBES data were acquired with a maximum swath angle of 120° and a frequency from 450 kHz to 210 kHz depending on water depth. Data were processed using the Teledyne PDS2000 and CARIS HIPS and SIPS software to produce a digital terrain model (DTM) and a backscatter mosaic of the seafloor that was mapped and described based on morphometric characterization. The DTM was characterized by: 0.2 m cell resolution up to 10 m depth; 0.5 m cell resolution at 10–20 m depth; 1.0 m cell resolution for depth >20 m. The acoustic data were calibrated, interpreted and properly validated based on 20 stations of ground-truthing for each study area, using a drop camera system (steel slide with high-definition camera and led light of 6000 lumen). Videos were analyzed using Adobe Premiere Pro software. The combination of SSS and MBES data was used to identify and map the RBs, as well as to evaluate their possible extent.

2.3. Data Collection

Three sites, distant about 500–1000 m one from the others, were randomly selected within the RBs identified and mapped at each study area with the acoustic surveys (Figure 1a–d). Three linear transects of 200 m each, distant about 50–100 m one from the others, were carried out at each site by using Remotely Operated Vehicle (ROV) (Table S1). Surveys were carried out on board the vessel *Issel* (property of CoNISMa—Consorzio Nazionale Interuniversitario per le Scienze del Mare), using the ROV *Prometeo*. The ROV was equipped with a low-definition camera for navigation and a 4 K video camera for the detailed observation of the rhodoliths, as well as a depth sensor, a compass for navigation, led lights with a maximum scene illumination of 13,000 lumen, a geographic positioning system and two laser beams for size and area measurements [68].

ROV videos were analysed using Adobe Premiere Pro software. Sequences with bad visibility, due to water turbidity or distance from the seabed, were discarded. A total of 20 frames were randomly extracted from each video transect. Each frame defined an area of 2.5 ± 0.2 m^2, according to the minimal area proposed by Weinberg [69] for the study of Mediterranean benthic communities and recently used for ROV imaging [57,68,70]. The rhodolith cover percentage and the proportion of living thalli were estimated for each frame by visual inspection as an approximate measure of the algal growth rate and vitality [37]. We considered as dead thalli those rhodoliths that where white or whitish in colour, based on expert judgement.

Visual inspections were validated through one quantitative sample per transect (3 samples per site), collected using a Van Veen grab (0.1 m^2 of surface and 0.02 m^3 of volume), according to the monitoring protocol for Mediterranean RBs developed within the MFSD [27]. Samples were sieved through a 0.5 mm mesh size. Living rhodolith thalli were sorted, dried with absorbent paper and preserved on-board in silica gel [38]. The taxa composing the algal nodules were identified at the lowest possible taxonomic level (i.e., species or genus).

Qualitative sub-samples of few rhodoliths were collected along each transect using Van Venn grab in order to perform algae taxonomic identification. Based on this data and on the general morphology of the rhodoliths samples, the overall contribution of each algal taxon to the total rhodolith cover percentage was estimated analysing the frames extracted from each video (20 frames per transect, 60 frames per site, 180 frames per area).

2.4. Taxonomic Identification

Calcareous algae were analysed by scanning electron microscopy (SEM) for detailed anatomical observation. Fragments of samples were sonicated using a Vitec sonicator (Carlsbad, CA, USA) to remove sediments, mounted on aluminium stubs with acrylic adhesive and coated with gold/palladium with a S150 Sputter Coater (Edwards, Crawley, UK) [71]. Then, observation was carried out using a LEICA Steroscan 430i scanning electron microscope (Leica, Cambridge, UK). The identification of non-geniculate red algae follows the most updated scientific literature, and algal taxonomy follows Algaebase [72].

2.5. Statistical Analysis

Statistical analyses were carried out using PRIMER v.6 software [73].

Permutational multivariate analysis of variance (PERMANOVA) [74] was used to test differences among algal assemblages at different spatial scales, based on the cover percentage of the species observed and identified, using the following hierarchical sampling design: Area (Ar, as random factor with 3 levels), Site (Si, as random factor with 3 levels) and Transect (Tr, as random factor with 3 levels), with $n = 20$ frames by each ROV video transect.

Data were analysed using the Bray-Curtis dissimilarity measure on untransformed data through 9999 permutations of residuals under a reduced model [75], while univariate analyses based on Euclidean distances [74] were performed on the rhodolith cover percentage and the proportion of living thalli. Mean squares calculated by PERMANOVA were used to estimate multivariate variance components associated at each spatial scale [76]. Non-metric multidimensional scaling (MDS) ordination plot was produced in order to visualize multivariate patterns in assemblages across scales. Furthermore, permutational analyses of multivariate dispersion (PERMDISP) were also performed to test the heterogeneity of multivariate dispersions among sites and among transects [77,78]. In order to detect which algal species contributed most to dissimilarity among the areas, a similarity percentage (SIMPER) routine was performed [79]. The assemblage structure of the different sites was then compared by plotting the cumulative dominance vs species rank in order to obtain k-dominance curves based on cover percentage [80].

3. Results

3.1. Mapping and Description of Rhodolith Beds

Habitat mapping activities allowed to identify areas characterized by rhodolith-forming algae, providing a reliable indication for the allocation of ROV transects and grab samplings. RBs showed a typical backscatter response characterized by a texture of bands of high and low signal, mostly due to the general patchiness of the habitat (Figure 2a). Areas characterized by higher cover of rhodoliths where identifiable by a higher backscatter, while low-cover RBs were not always distinguishable from detritic seabed without rhodoliths, such as the coastal detritic biocoenosis [49]. Based on acoustic data validated by visual surveys, we identified high-density RBs as those with a higher backscatter, corresponding to a cover broadly higher than 20–30%. On the contrary, areas with a lower backscatter and mostly characterized by a cover of 10% or less, often interspersed with high-density RBs, were considered low-density RBs. Coralligenous bioconstructions and muddy bottoms were also easily distinguishable based on the backscatter (Figure 2a).

Consistently with both SSS and MBES backscatter, rhodoliths were observed in all the ROV transects and grab samples, within the four study areas. RBs (*sensu* [6,17]) were observed at Tremiti Islands MPA, off Gallipoli and at Armeleia shoal. On the contrary, only occasional and densely-branched nodules of *Lithophyllum racemus*, characterized by short ramifications, were found northwest Otranto from 38 to 44 m depth (Table 1). For this reason, this latter area was not included in the analysis.

The RB at Tremiti Islands MPA was patchy distributed around the archipelago as a mosaic of rhodoliths and coralligenous, and as RB *sensu stricto* from 15 to 48 m depth. The RB covered a total surface of 2.47 km^2 (1.70 km^2 of high-density RB) and was present in both the B and C zones of the MPA, such as the highly protected and the partially protected zone, respectively (Figure 2b). The most common morphotypes were pralines and boxworks, mainly of *L. racemus* and *Neogoniolithon brassica-florida* (Figure 3; Figure 4a–d), respectively. *Spongites fruticulosus*, *Titanoderma pustulatum*, *Lithothamnion crispatum*, *Mesophyllum* sp., *Lithothamnion minervae* and *L. valens* were also present (Table 1; Figure 4e–h).

The RB off Gallipoli was found between 36–45 m depth, mainly as a mosaic of rhodoliths and coralligenous habitat (i.e., RB and patchy coralligenous outcrops). The RB covered an area of 4.04 km^2 (2.90 km^2 of high-density RB) (Figure 2c) and was dominated by unattached branches morphotype (Figure 3). Rhodoliths were characterized by short and numerous branches (mostly *L. racemus*), or by

few, long and thin ramifications (e.g., *Lithothamnion corallioides*). The dominant species was *L. racemus* (Figure 4i–l), while *L. corallioides*, *L. crispatum* and *T. pustulatum* were less abundant in terms of cover percentage (Table 1).

At Armeleia shoal, RB bathymetrically followed some coralligenous formations, between 35 and 41 m depth, covering an area of 2.61 km² (2.11 km² of high-density RB) (Figure 2d). Rhodoliths were mainly unattached branches (Figure 3), with the dominance of *L. corallioides* (Figure 4m–p) and the occasional occurrence of *L. minervae*, *L. crispatum*, *Mesophyllum* sp., and *T. pustulatum* (Table 1).

The rhodolith cover percentage in Armeleia was larger than the coverages found in Tremiti and in Gallipoli (Table 1), while the proportion of living thalli was higher in Tremiti than Gallipoli and Armeleia (Table 2). Both the rhodolith cover percentage and the proportion of living thalli showed significant differences at the scales of transects and sites (Table 2). PERMDISP analyses revealed significant differences in multivariate dispersion across scales, both across transects (rhodolith cover percentage: F= 6.765 (p = 0.0001); proportion of living thalli: F: 6.650 (p = 0.0001)) and sites (rhodolith cover percentage F= 6.891 (p = 0.0001); proportion of living thalli: F= 14.842 (p = 0.0001)).

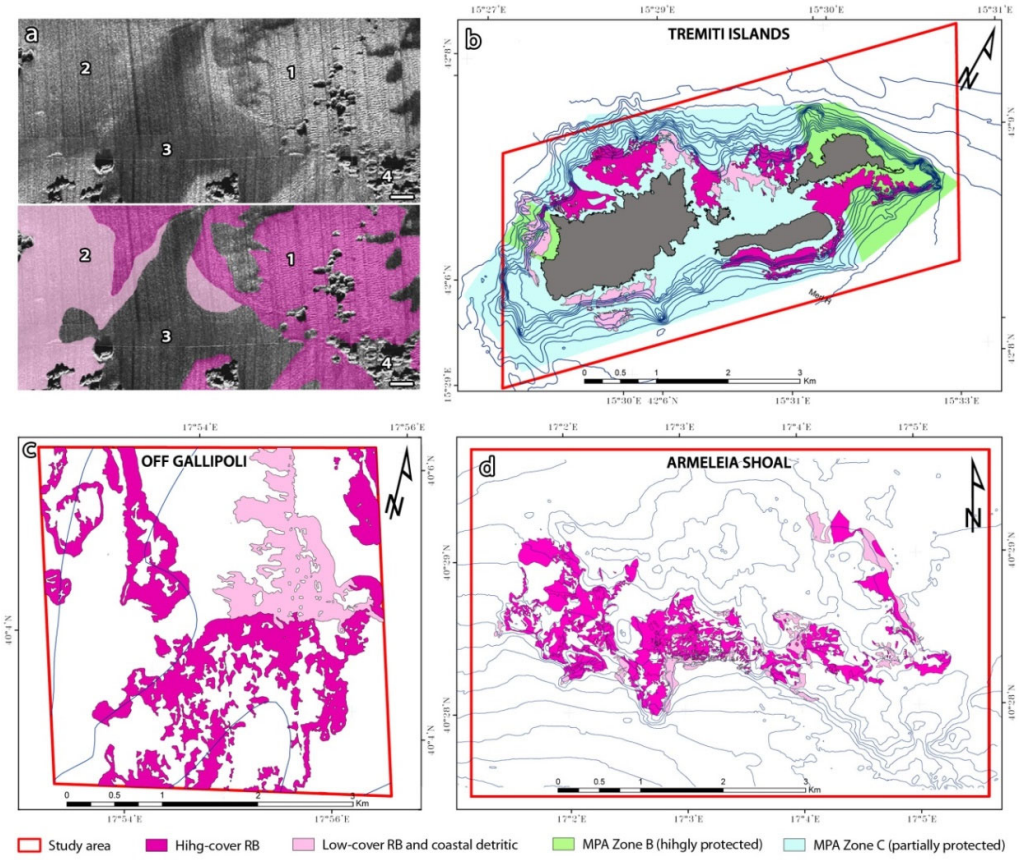

Figure 2. Mapping of rhodolith beds (RBs): (**a**) Example of backscatter at Armeleia shoal and habitat interpretation, with: high-cover RB (1) in an area characterized by mega-ripples, low-cover RB and coastal detritic (2), muddy-detritic bottom (3), and coralligenous bioconstructions (4) (scale bar 10 m); (**b**) RB at Tremiti Islands, with indication of the Marine Protected Area (MPA) zonation; (**c**) RB off Gallipoli; (**d**) RB at Armeleia Shoal.

Table 1. Mean cover percentage and standard deviation of each rhodolith-forming species observed in the four study areas, with indication of total cover percentage and the proportion of living thalli for each area.

Taxa	Northwest Otranto	Tremiti Islands	Off Gallipoli	Armeleia Shoal
Lithophyllum racemus (Lamarck) Foslie	<2	18.59 ± 16.09	22.25 ± 13.31	
Lithothamnion corallioides (P. Crouan & H. Crouan) P. Crouan & H. Crouan			0.73 ± 0.45	59.19 ± 20.68
Lithothamnion crispatum Hauck		2.55 ± 2.71	0.73 ± 0.45	1.78 ± 1.72
Lithothamnion minervae Basso		0.22 ± 0.47		2.64 ± 2.43
Lithothamnion valens Foslie		0.11 ± 0.33		
Mesophyllum sp.		1.30 ± 1.16		1.75 ± 1.34
Neogoniolithon brassica-florida (Harvey) Setchell & Mason		12.36 ± 14.06		
Spongites fruticulosus Kützing		4.91 ± 5.54		
Titanoderma pustulatum (J.V. Lamourou) Nägeli		3.23 ± 3.59	0.74 ± 0.44	0.11 ± 0.48
Cover %		43.27 ± 30.53	24.44 ± 14.09	65.59 ± 19.57
Live/Dead rhodolith ratio		78.25 ± 11.45	73.18 ± 9.54	50.95 ± 24.89

Table 2. Results of PERMANOVAs testing for spatial differences in the proportion of living thalli and the rhodolith cover percentage at scales of area, site and transect. Estimates of multivariate variation are given for each spatial scale. df = degrees of freedom; MS = mean sum of squares; Pseudo-F = F value by permutation; p (perm) = *p*-values based on 9999 random permutations of appropriate units.

		Proportion of Living Thalli				Rhodolith Cover			
Source	**df**	**MS**	**Pseudo-F**	**p (perm)**	**Variation Components**	**MS**	**Pseudo-F**	**p (perm)**	**Variation Components**
Ar	2	35,194.0	2.955	0.0943	185.52	43,479.0	1.919	0.1619	165.92
Si(Ar)	4	12,397.0	11.162	0.0002 *	188.14	23,582.0	11.426	0.0002 *	358.70
Tr(Si(Ar))	14	1097.0	5.811	0.0001 *	45.99	2038.5	6.644	0.0001 *	87.68
Res	394	188.8			188.77	306.8			306.82
Total	414								

* $p < 0.001$.

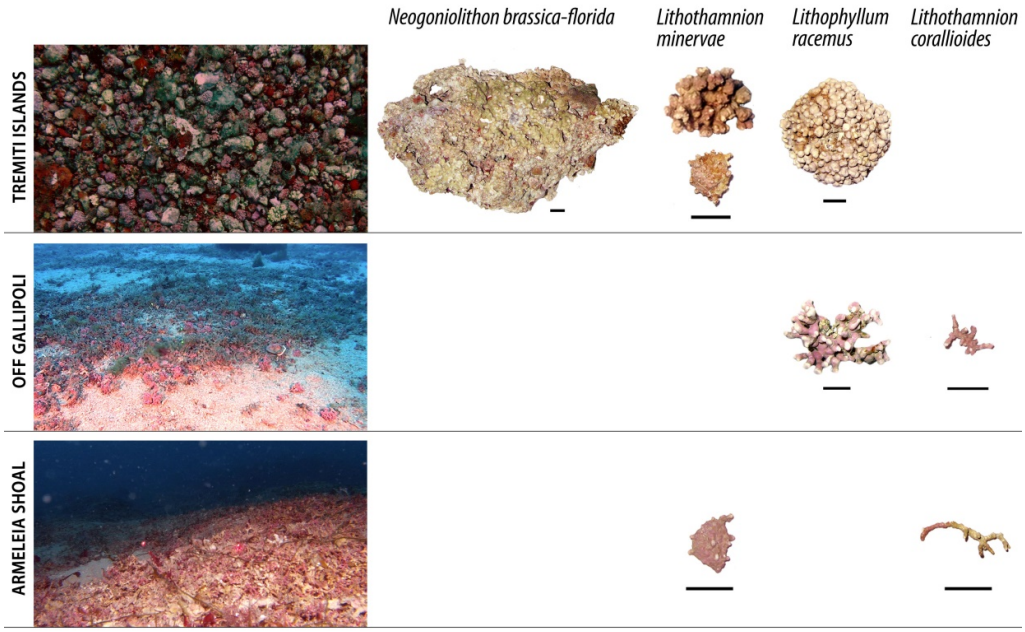

Figure 3. The three rhodolith beds identified, with detail of the morphotypes of four main species collected (pralines and boxwork at Tremiti Islands, unattached branches off Gallipoli and at Armeleia Shoal). Scale bars: 1 cm.

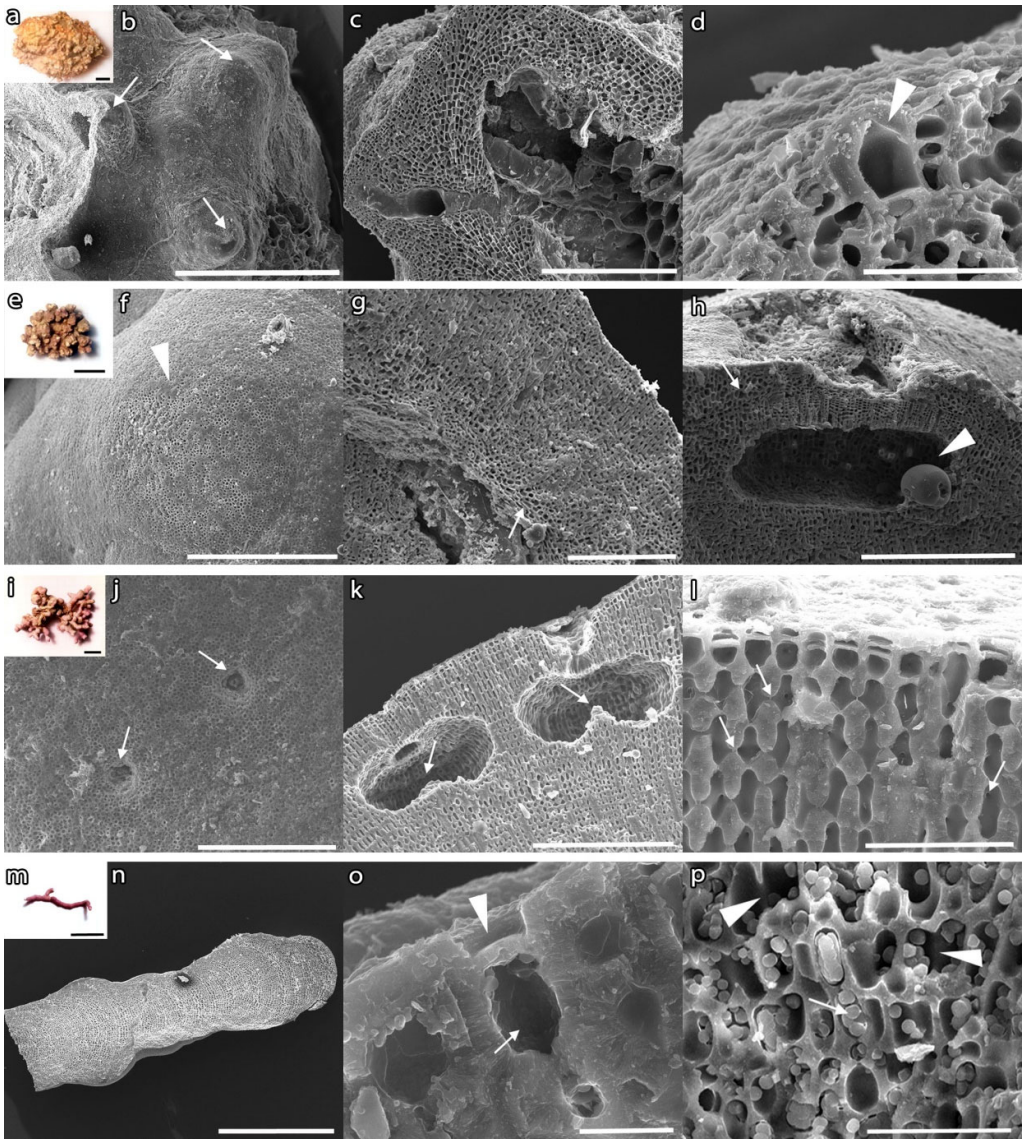

Figure 4. Examples of morphology and inner structure of the four main rhodolith species collected: (**a**) Boxwork of *Neogoniolithon brassica-florida* from Tremiti Islands (scale bar 1 cm) with: (**b**) protruding conical uniporate conceptacles (arrows) (scale bar 2 mm); (**c**) section of the thallus with monomerous construction (scale bar 500 μm); (**d**) terminal trichocyte cell (arrowheads) (scale bar 50 μm). (**e**) Fruticose praline of *Lithothamnion minervae* from Tremiti Islands (scale bar 1 cm) with: (**f**) multiporate conceptacle in surface view (arrowhead) (scale bar 400 μm); (**g**) section of the thallus with monomerous construction and non-coaxial growth (arrow) (scale bar 200 μm); (**h**) multiporate conceptacle (arrowhead) overgrown by new cortical filaments (arrow) (scale bar 300 μm). (**i**) Unattached branch of *Lithophyllum racemus* from Gallipoli (scale bar 1 cm), with: (**j**) Epithallus in surface view with pores of uniporate sporangial conceptacles (arrows) (scale bar 400 μm) and (**k**) a central columella raising from the floor (arrows) (scale bar 300 μm); (**l**) section with cortical cells joined laterally by secondary pit-connections (arrow) (scale bar 50 μm). (**m**) Unattached branch of *Lithothamnion corallioides* from Armeleia Shoal (scale bar 1 cm) with: (**n**) section of a branch (scale bar 1 mm); (**o**) section showing a flared epithallial cell (arrowhead) and elongated subepithallial cell

(arrow) (scale bar 10 μm); (**p**) cells of neighboring filaments linked by lateral cell fusions (arrowheads), with cells containing starch grains (arrows) (scale bar 50 μm).

3.2. Heterogeneity of Rhodolith Beds

The PERMANOVA analysis highlighted significant differences in the algal cover percentage from the three RBs studied, at all the considered scales (Table 3). In addition, estimates of multivariate variation showed the largest variation at area scale, followed by residual variation, indicating multivariate heterogeneity among sampling units, whereas the contributions of site and transect scales resulted marginal (Table 3; Figure 5).

Table 3. Results of PERMANOVAs testing for spatial differences in structure of algal assemblages at area (Ar), site (Si) and transect (Tr) scales, based on the algal cover percentage from ROV imaging. Analyses based on Bray-Curtis dissimilarities from untransformed data. Estimates of multivariate variation are given for each spatial scale. df = degrees of freedom; MS = mean sum of squares; Pseudo-F = F value by permutation; p (perm) = *p*-values based on 9999 random permutations of appropriate units. * $p < 0.05$; *** $p < 0.001$.

Source	df	MS	Pseudo-F	p (perm)	Variation Components
Ar	2	382,000	16.25	*	2858.60
Si(Ar)	4	24,471.00	5.80	***	337.68
Tr(Si(Ar))	14	4166.70	5.64	***	173.55
Res	394	739.04			739.04
Total	414				

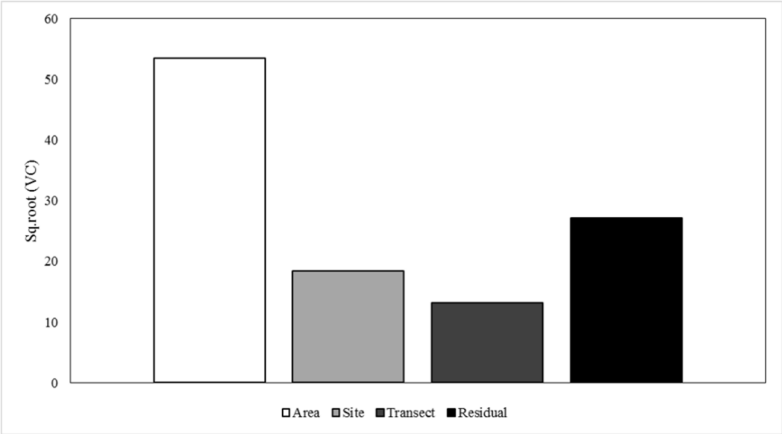

Figure 5. Square root of multivariate variance components (VC) at each spatial scale for all the algal species.

MDS plot revealed important differences between the assemblage of Armeleia shoal and the other two areas. Pearson correlations coefficients (>0.6) indicated that the observed differences were driven by *L. minervae* and *L. corallioides*, which mainly characterized the assemblages from Armeleia shoal, whereas RBs from Tremiti Islands and Gallipoli were mainly characterized by *L. racemus* (Figure 6). Higher variability among replicates was also observed at Tremiti Islands MPA and Gallipoli, compared to Armeleia shoal (Figure 6).

Results of PERMDISP showed significant differences in multivariate dispersion across scales. More specifically, significant differences in the spatial heterogeneity of assemblages across transects ($F = 11.396$ [$p = 0.0001$]) and sites ($F = 26.588$ [$p = 0.0001$]) were observed (Figure 7a,b).

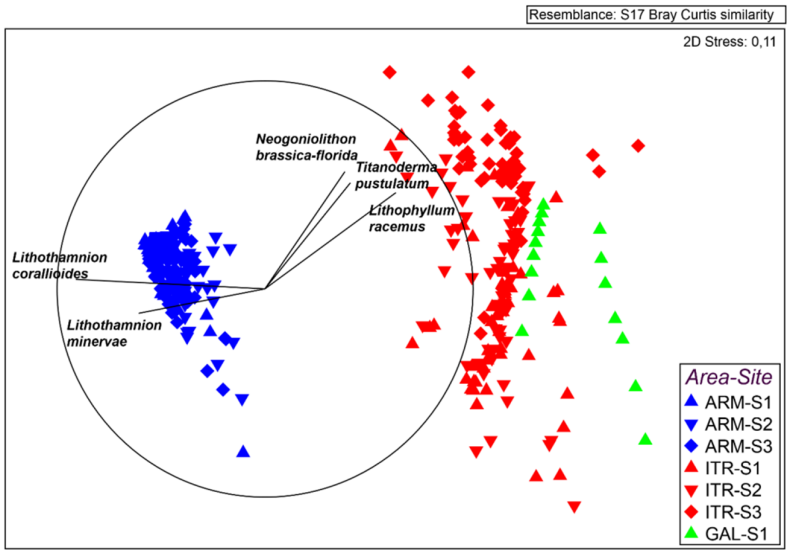

Figure 6. MDS plots on the basis of all the rhodoliths species found in the different study areas (ARM: Armeleia shoal; ITR: Tremiti Islands; GAL: Gallipoli).

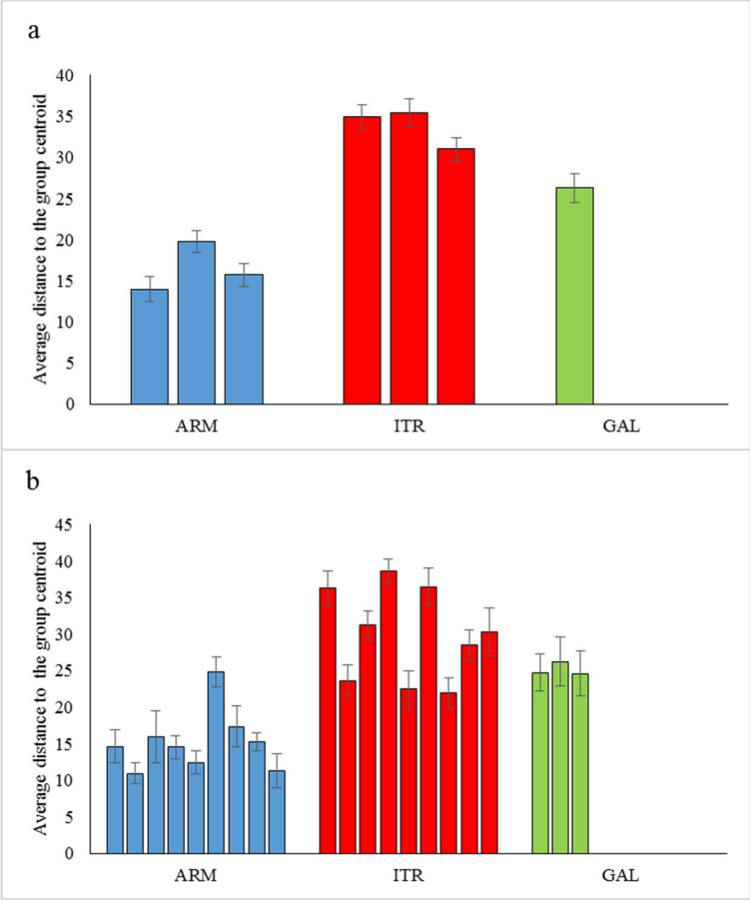

Figure 7. Multivariate dispersion (PERMDISP). Patterns of variability of algal assemblages: (**a**) across transects and (**b**) within sites, split for the different areas (ARM: Armeleia shoal; ITR: Tremiti Islands; GAL: Gallipoli, where a rhodolith bed was found only in one of the three study sites). Error bars represent standard error.

The SIMPER analysis revealed a high dissimilarity in the algal assemblages among the study areas, reaching the 97% between Gallipoli vs Armeleia (Table 4). RBs from Armeleia shoal and Tremiti Islands MPA were also characterized by the patchy presence of green seaweeds belonging to the family Caulerpaceae, settled on the rhodoliths and locally abundant. For this reason, Caulerpaceae have been included in the SIMPER analysis. In particular, *Caulerpa prolifera* was found only at Tremiti Islands MPA (0.4%), while *C. cylindracea* both at Armeleia shoal (4.58%) and Tremiti Islands MPA (8.12%) (Table 4).

Table 4. Results of SIMPER analysis. Average cover percentage of algal taxa contributing to most of the Bray-Curtis dissimilarity among areas. ARM: Armeleia shoal; ITR: Tremiti Islands; GAL: Gallipoli). Av = Average cover percentage; Av.Diss = Average dissimilarity; Contrib% = Contribution (%).

	ARM	ITR	GAL	ARM vs. ITR 94.70%		ARM vs. GAL 96.86%		ITR vs. GAL 64.33%	
Taxa	**Av.**	**Av.**	**Av.**	**Av.Diss**	**Contrib%**	**Av.Diss**	**Contrib%**	**Av.Diss**	**Contrib%**
L. corallioides	59.19	0.00	0.73	51.78	54.68	61.42	63.41	1.17	1.82
L. racemus	0.00	18.59	22.25	14.26	15.05	23.33	24.08	26.09	40.55
C. cylindracea	4.58	8.12	0.0	7.50	7.92	4.70	4.85	7.50	11.66
N. brassica-florida	0.00	12.37	0.00	9.24	9.76	0.00	0.00	15.11	23.49
S. fruticulosus	0.00	4.91	0.00	3.61	3.81	0.00	0.00	5.77	8.97
L. minervae	2.64	0.00	0.00	2.59	2.74	3.18	3.28	0.00	0.00
T. pustulatum	0.00	3.23	0.73	2.50	2.64	0.78	0.81	3.17	4.93
L. crispatum	1.78	2.55	0.73	1.93	2.04	1.34	1.39	3.41	5.29
Mesophyllum sp.	1.75	1.30	0.00	1.10	1.16	2.12	2.19	1.86	2.88
C. prolifera	0.00	0.40	0.00	0.20	0.21	0.00	0.00	0.26	0.41

K-dominance curves showed that rhodolith taxa dominance at Gallipoli and Armeleia markedly differs from curves of Tremiti Islands MPA, this latter being characterized by less dominant taxa (Figure 8). At Armeleia shoal the most abundant species in terms of cover was *L. corallioides*, with a dominance of 90% approximately. On the contrary, *L. racemus* resulted the dominant species at Gallipoli and Tremiti Islands MPA, with a dominance of 90% and 40–60%, respectively.

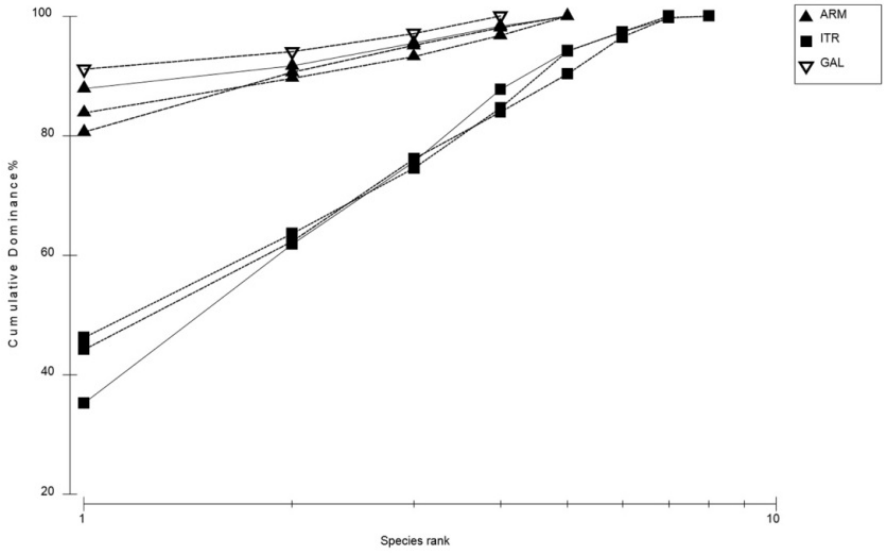

Figure 8. K-dominance curves for rhodolith species abundances (in terms of cover percentages) in the different sites of the three study areas (ARM: Armeleia shoal; ITR: Tremiti Islands; GAL: Gallipoli).

4. Discussion

4.1. Rhodolith Beds Variability from Small to Large Scale

The combination of visual surveys and acoustic data represented the best approach for the identification of RBs, and the high backscatter registered in association with this habitat was in

accordance with recent literature (e.g., [8,67,81]). However, backscatter can vary according to many factors such as, among the others, incident angle, sediment type, grain size, seabed slope and roughness [81,82], thus ground truth is essential for a proper interpretation.

The adoption of a hierarchical nested design for the analysis of spatial patterns based on ROV imaging and samples over small (~10^{-1} m) to large (~10^{6} m) spatial scales allowed to investigate the composition of the newly-identified rhodolith assemblages across the coast of Apulia (Central Mediterranean Sea). Multivariate analyses highlighted significant differences in the rhodolith assemblages at all the considered scales, with the largest variation among areas. These differences are driven by four main species, such as *L. minervae*, *L. corallioides*, *L. racemus* and *N. brassica-florida* (Figure 3; Table 4). The analysis of multivariate variation showed that areas added a significant contribution of variance above that of sampling units that are, however, also contributing to the overall variability. This variability at area level is likely due to the distance and the environmental differences among each area, underlining a strong heterogeneity and the presence of specific rhodolith communities in the different areas. Rhodoliths were also characterized by significant differences at the smaller scales in both rhodolith cover percentage and proportion of living thalli (Table 2). In addition, wave-induced turbulence, light intensity and sedimentation together with depth range, can represent environmental drivers determining the presence, structure and functioning of rhodolith beds [83]. Moreover, fishing activities can also influence the size and the morphology of the rhodoliths.

Our result further reinforces the idea that small-scale processes are as important as large-scale ones in generating patterns in rhodolith assemblages, as also observed in other marine habitats such as intertidal and subtidal turfing algal assemblages, soft-sediment macrofauna and rocky shore communities [42,43,84,85]. Moreover, our results confirm that Mediterranean RBs are featured by complex spatial patterns and a high diversity of shapes and morphologies, determining a substantial heterogeneity.

The principal ecosystem engineers and the main contributor in dissimilarities were *L. racemus* and *L. corallioides*, the latter included in the Annex V of the EU Habitat Directive [29]. In particular, *L. racemus* was the dominant species in all the study areas except from Armeleia shoal, where *L. corallioides* was dominant. The rhodolith assemblage was particularly heterogeneous at Tremiti Islands MPA where, despite the large cover of *L. racemus* and *N. brassica-florida*, it was not observed the marked dominance of one species. RBs shallower than 25 m depth, as Tremiti's one, are also rather uncommon in the Mediterranean basin, being mainly present in the northern Adriatic Sea and in the Gulf of Gabés (Eastern Mediterranean, Tunisia) [25]. Indeed, most Mediterranean RBs known thus far occur between 30 and 75 m, although they have been broadly found from 9 to 150 m of depth [25].

4.2. Rhodolith Morphotypes and Main Hydrodynamic Regime

The clear separation of Armeleia shoal from the other two areas (Figure 6) suggested that a combination of environmental drivers (e.g., currents and sedimentation) possibly shaped a different rhodolith assemblage in this area in terms of species composition, rhodolith growth forms and cover. Besides temperature, wind waves, nutrients and irradiance levels as a function of photosynthesis, calcification and respiration process [86–88], bottom currents represent important variables governing rhodolith occurrence and development. In fact, different hydrodynamic regimes can influence RB composition and rhodolith morphotype [33,89]. In particular, spherical and densely-branched rhodoliths seem to be typical of exposed sites (i.e., subject to strong bottom currents), while open-branched rhodoliths are found in more stable environments (i.e., subject to moderate bottom currents) [22,23,44]. The dominant presence of pralines and boxworks at Tremiti Islands MPA could be due to the relevant exposure of the archipelago to strong water currents coming from the north Adriatic [55–57]. Both densely-branched rhodoliths (*L. racemus*) and open-branched ones (*L. corallioides*) were observed off Gallipoli. This variety may be driven by the different local conditions due to the presence of large coralligenous outcrops scattered on the coastal detritic bottom with RBs (mosaic of coralligenous and RBs) that may affect water masses movements on the seabed. Finally, RBs at Armeleia shoal were mainly characterized by unattached branches with few, long and thin ramifications, likely due to a more hydrodynamically stable environment [53,66]. These results

seemed to support the hypothesis that Mediterranean RBs are mainly present around islands and capes (as Tremiti Islands), around banks and shoals (as Armeleia shoal), as well as on top of submarine plateau and on marine terraces (as off Gallipoli) [25].

4.3. Threats and Conservation

Habitats featured by high variability of assemblages and complex patterns of distribution require different protected sites for a representative conservation policy. Heterogeneity in rhodolith species composition, morphologies and cover resulted locally very high in all the RBs, representing eligible sites for conservation measures, such as the institution and/or the implementation of Natura2000 sites according to the EU Habitat Directive [29]. To that regard, areas as Armeleia shoal are good candidates for strategic protection initiatives due to the co-existence of priority habitats [27,29], such as coralligenous bioconstructions and RBs.

The observed high patchiness of the rhodolith assemblage at Tremiti Islands could be enhanced by a number of anthropic stressors including high touristic frequentation, anchoring activities and some fishing practices that occur in the area [47,57], albeit no evident signs of destructive fishing practices (e.g., trawl marks) have been observed on the RB. However, trawling is allowed only below 50 m depth in the Mediterranean Sea and our survey was carried out mostly shallower than this depth, so it is assumed that no trawling activities are carried out on the studied RBs. Beside the direct effect of fishing activities, the indirect human pressures might negatively influence the habitats as reported along the Tyrrhenian coasts where the great amount of marine litter was found to affect seabed [90] and litter abundance was negatively correlated to rhodolith cover [91]. However, the conservation status of RBs in a 25-year-old no-take area of the north-western Mediterranean (Columbretes Islads Marine Reserve) [92] underlined a beneficial protection from fishing activities on RBs cover and species richness, although the proportion of living rhodoliths was similar in protected and in unprotected areas.

Further evidences of human pressures could be highlighted by the presence of the green algae *Caulerpa cylindracea*. This alien and invasive species was frequently observed in many sites, and resulted locally very common at Tremiti Islands MPA. Local heavy overgrowth of *C. cylindracea* on RBs may be facilitated by anthropogenic impacts [93] and it could affect the rhodolith assemblage [94,95]. In particular, besides the shading due to the settling on the rhodoliths, *C. cylindracea* may significantly influence the quantity and biochemical composition of sedimentary organic matter across the RBs [96,97].

The ongoing ocean acidification and rising of water temperature might hamper the formation of RBs in the near future or result in the degradation of present assemblages [98–103]. As recently highlighted for other calcifying habitat formers such as cold-water corals [3,104], knowledge about patterns of distribution and main habitat features are fundamental to assess ongoing and future changes [105]. Understanding the status of RBs without consistent information about species compositions, dominant morphologies, proportion of living thalli, habitat features and disturbances (both natural and anthropogenic) shaping presence and distribution of RBs is very unlikely. This information, together with the assessment of RBs sensitivity to human disturbance, is essential for the proper protection and management of this productive marine habitat.

5. Conclusions

Our results showed the potential of applying coordinated monitoring at regional and national level that, in the near future, could confirm the presence of complex spatial and diversity patterns possibly driven by a combination of natural processes and anthropic pressures (e.g., organic inputs, coastal human activities, fishing pressures). Visual techniques proved to be effective, but sampling is still needed for taxonomic identification and for both calibration and validation of remotely-collected data (both geophysical and visual). The identification of strategic areas which are as representative as possible of the different Mediterranean RBs is essential, together with the application of *ad hoc* conservation measures to protect this unique marine habitat.

Supplementary Materials: The following are available online at www.mdpi.com/2077-1312/8/10/813/s1, Table S1. Coordinates and depth range of the ROV transects carried out in the four study areas, with three sites per area and three transects per site.

Author Contributions: Conceptualization, G.C., L.R., S.K., A.F., S.F. and F.M.; methodology, G.C., L.R., S.K., A.F., S.F., F.D.G. and F.M.; software, G.C., L.R., S.F. and F.D.G.; validation, G.C., L.R., S.K., A.F., S.F., A.T., E.B., N.U. and F.M.; formal analysis, L.R. and S.F.; investigation, G.C., S.K., A.F. and F.M.; resources, G.C., A.F., A.T. and F.M.; data curation, G.C. and S.K.; writing—original draft preparation, G.C., L.R., S.K., A.F., S.F. and F.M.; writing—review and editing, G.C., L.R., S.K., A.F., S.F., A.T. and F.M.; visualization, G.C., L.R., S.K., A.F. and F.D.G.; supervision, A.F., S.F. and F.M.; project administration, A.T. and F.M.; funding acquisition, A.T., E.B., N.U. and F.M. All authors have read and agreed to the published version of the manuscript.

Funding: This research was funded by the Italian Ministry of Education, University and Research (Ministero dell'Istruzione, dell'Università e della Ricerca; Programma Operativo Nazionale—PON 2014–2020), grant AIM 1807508-1, Linea 1, and by the Italian Ministry for Environment, Land and Sea Protection (Ministero dell'Ambiente e della Tutela del Territorio e del Mare) as part of the Italian monitoring program for the implementation of the Marine Strategy Framework Directive (European Union, 2008/56/EC).

Conflicts of Interest: The authors declare no conflict of interest. The funders had no role in the design of the study; in the collection, analyses, or interpretation of data; in the writing of the manuscript, or in the decision to publish the results.

References

1. Crain, M.C.; Kroeker, K.; Halpern, B.S. Interactive and cumulative effects of multiple human stressors in marine systems. *Ecol. Lett.* **2008**, *11*, 1304–1315.
2. Vinebrooke, R.D.; Cottingham, K.L.; Norberg, J.; Scheffer, M.; Dodson, S.I.; Maberly, S.C.; Sommer, U. Impacts of multiple stressors on biodiversity and ecosystem functioning: The role of species co-tolerance. *Oikos* **2004**, *104*, 451–457.
3. Chimienti, G.; Bo, M.; Mastrototaro, F. Know the distribution to assess the changes: Mediterranean cold-water coral bioconstructions. *Rend. Lincei Sci. Fis. Nat.* **2018**, *29*, 583–588.
4. Zajac, R.M.; Vozarik, J.M.; Gibbons, B.R. Spatial and temporal patterns in macrofaunal diversity components relative to sea floor landscape structure. *PLoS ONE* **2013**, *8*, e65823.
5. Jones, C.G.; Lawton, J.H.; Shachak, M. Organisms as ecosystem engineers. *Oikos* **1994**, *69*, 373–386.
6. Steller, D.L.; Riosmena-Rodriguez, R.; Foster, M.S.; Roberts, C.A. Rhodolith bed diversity in the Gulf of California: The importance of rhodolith structure and consequences of disturbance. *Aquat. Conserv.* **2003**, *13*, S5–S20.
7. Ingrosso, G.; Cecchi, L.; Bertolino, M.; Bevilacqua, S.; Bianchi, C.N.; Bo, M.; Boscari, E.; Cardone, F.; Cattaneo-Vietti, R.; Cau, A.; et al. Mediterranean Bioconstructions along the Italian Coast. *Adv. Mar. Biol.* **2018**, *79*, 61–136.
8. Sañé, E.; Chiocci, F.L.; Basso, D.; Martorelli, E. Environmental factors controlling the distribution of rhodoliths: An integrated study based on seafloor sampling, ROV and side scan sonar data, offshore the W-Pontine Archipelago. *Cont. Shelf Res.* **2016**, *129*, 10–22.
9. Grall, J.; Glemarec, M. Biodiversite des fonds de maërl en Bretagne: Approache fonctionnelle et impacts anthropogeniques. *Vie Milieu* **1997**, *47*, 339–349.
10. Foster, M.S.; Filho, G.M.A.; Kamenos, K.A.; Riosmena-Rodríguez, R.; Steller, D.L. Rhodoliths and rhodolith beds. In *Research and Discoveries: The Revolution of Science Through SCUBA*; American Academy of Underwater Sciences: Mobile, AL, USA, 2013; pp. 143–155.
11. Ordines, F.; Bauzá, M.; Sbert, M.; Roca, P.; Gianotti, M.; Massutí, E. Red algal beds increase the condition of nekto-benthic fish. *J. Sea Res.* **2015**, *95*, 115–123.
12. Riosmena-Rodríguez, R.; Nelson, W.; Aguirre, J. (Eds.) *Rhodolith/Maërl Beds: A Global Perspective*; Coastal Research Library 15; Springer: Cham, Switzerland, 2017; pp. 1–362.
13. Jacquotte, R. Etude des fonds de maerl de Méditerranée. *Recueil Travaux StationMarine d'Endoume* **1962**, *26*, 141–216.
14. Hall-Spencer, J.M.; Grall, J.; Moore, P.G.; Atkinson, R.J.A. Bivalve fishing and maerl-bed conservation in France and the UK-retrospect and prospect. *Aquat. Conserv.* **2003**, *13*, S33–S41.

15. Barberá, C.; Moranta, J.; Ordines, F.; Ramón, M.; de Mesa, A.; Díaz-Valdés, M.; Grau, A.M.; Massutí, E. Biodiversity and habitat mapping of Menorca Channel (western Mediterranean): Implications for conservation. *Biodivers. Conserv.* **2012**, *21*, 701–728.
16. Cavalcanti, G.S.; Gregoraci, G.B.; Santos, E.O.; Silveira, C.B.; Meirelles, P.M.; Longo, L.; Gotoh, K.; Nakamura, S.; Iida, T.; Sawabe, T.; et al. Physiologic and metagenomic attributes of the rhodoliths forming the largest $CaCO_3$ bed in the South Atlantic Ocean. *ISME J.* **2014**, *8*, 52–62.
17. Basso, D.; Babbini, L.; Kaleb, S.; Bracchi, V.; Falace, A. Monitoring deep Mediterranean rhodolith beds. *Aquat. Conserv.* **2016**, *26*, 549–561.
18. Krayesky-Self, S.; Schmidt, W.; Phung, D.; Henry, C.; Sauvage, T.; Camacho, O.; Felgenhauer, B.E.; Fredericq, S. Eukaryotic life inhabits rhodolith-forming coralline algae (Hapalidiales, Rhodophyta), remarkable marine benthic microhabitats. *Sci. Rep.* **2017**, *7*, 45850.
19. Coletti, G.; Basso, D.; Frixa, A. Economic importance of coralline carbonates. In *Rhodolith/Maërl Beds: A Global Perspective*; Riosmena-Rodríguez, R., Nelson, W., Aguirre, J., Eds.; Coastal Research Library—Springer: Cham, Switzerland, 2017; Volume 15, pp. 87–101.
20. Schubert, N.; Schoenrock, K.M.; Aguirre, J.; Kamenos, N.A.; Silva, J.; Horta, P.A.; Hofmann, L.C. Coralline algae: Globally distributed ecosystem engineers. *Front. Mar. Sci.* **2020**, *7*, 352.
21. Peña, V.; Barbara, I. Maerl community in the north-west Iberian Peninsula: A review of floristic studies and long-term changes. *Aquat. Conserv.* **2008**, *18*, 339–366.
22. Sciberras, M.; Rizzo, M.; Mifsud, J.R.; Camilleri, K.; Borg, J.A.; Lanfranco, E.; Schembri, P.J. Habitat structure and biological characteristics of a maerl bed off the northeastern coast of the Maltese Islands (central Mediterranean). *Mar. Biodivers.* **2009**, *39*, 251–264.
23. Di Geronimo, R.; Giaccone, G. Le alghe calcaree nel detritico costiero di Lampedusa (Isole Pelagie). *Boll. Accad. Gioenia Sci. Nat.* **1994**, *27*, 5–25.
24. Falace, A.; Kaleb, S.; Agnesi, S.; Annunziatellis, A.; Salvati, E.; Tunesi, L. Macroalgal composition of rhodolith beds in a pilot area of the Tuscan Archipelago (Tyrrhenian Sea): Primary elements to evaluate the degree of conservation of this habitat. In Proceedings of the 2nd Mediterranean Symposium on the conservation of Coralligenous & other Calcareous Bio-Concretions, Portorož, Slovenia, 29–30 October 2014; pp. 213–214.
25. Basso, D.; Babbini, L.; Ramos-Esplá, A.A.; Salomidi, M. Mediterranean Rhodolith Beds. In *Rhodolith/Maërl Beds: A Global Perspective*; Riosmena-Rodríguez, R., Nelson, W., Aguirre, J., Eds.; Coastal Research Library—Springer: Cham, Switzerland, 2017; Volume 15, pp. 281–298.
26. Rendina, F.; Kaleb, S.; Caragnano, A.; Ferrigno, F.; Appolloni, L.; Donnarumma, L.; Russo, G.F.; Sandulli, R.; Roviello, V.; Falace, A. Distribution and characterization of deep rhodolith beds off the Campania coast (SW Italy, Mediterranean Sea). *Plants* **2020**, *9*, 985.
27. European Parliament. Council of the European Union Directive 2008/56/EC of the European Parliament and of the Council of 17 June 2008 establishing a framework for Community action in the field of marine environmental policy (Marine Strategy Framework Directive). *Off. J. Eur. Union* **2008**, *L164*, 19.
28. European Commission. Commission decision of 1 September 2010 on criteria and methodological standards on good environmental status of marine waters. *Off. J. Eur. Union* **2010**, *L232*, 14.
29. European Parliament. Council directive 1992/43/EC Conservation of natural habitats and of wild fauna and flora. *Off. J. Eur. Union* **1992**, *L206*, 7–50.
30. European Community. Council Decision 82/72/EEC of 3 December 1981 concerning the conclusion of the Convention on the conservation of European wildlife and natural habitats (Bern Convention). *Off. J. Eur. Union* **1982**, *L38,* 1–2.
31. European Parliament. Council Regulation No. 1967/2006 concerning management measures for the sustainable exploitation of fishery resources in the Mediterranean Sea, amending Regulation (EEC) No 2847/93 and repealing Regulation (EC) No 1626/94. *Off. J. Eur. Union* **2006**, *L409*, 11.
32. United Nations Environmental Program. *Proposal of Standard Methods for Inventorying and Monitoring Coralligenous and Rhodoliths Populations*; UNEP(DEPI)/MED WG.359/10; RAC/SPA: Tunis, Tunisia, 2011; pp. 1–23.
33. Steller, D.L.; Foster, M.S. Environmental factors influencing distribution and morphology of rhodoliths in Bahía Concepción, B.C.S., México. *J. Exp. Mar. Biol. Ecol.* **1995**, *194*, 201–212.

34. Steller, D.L.; Hernández-Ayón, J.M.; Riosmena-Rodríguez, R.; Cabello-Pasini, A. Effect of temperature on photosynthesis, growth and calcification rates of the free-living coralline alga *Lithophyllum margaritae*. *Ciencias Mar.* **2007**, *33*, 441–456.
35. Nelson, W.; Neill, K.; Farr, T.; Barr, N.; D'Archino, R.; Miller, S.; Stewart, R. *Rhodolith Beds in Northern New Zealand: Characterisation of Associated Biodiversity and Vulnerability to Environmental Stressors*; New Zealand Aquatic Environment and Biodiversity Report; Ministry for Primary Industries: Wellington, New Zeland, 2012; pp. 1–106.
36. Barberá, C.; Bordehore, C.; Borg, J.A.; Glemarec, M.; Grall, J.; Hall-Spencer, J.M.; De la Huz, C.; Lanfranco, E.; Lastra, M.; Moore, P.G.; et al. Conservation and management of northeast Atlantic and Mediterranean maërl beds. *Aquat. Conserv.* **2003**, *13*, S65–S76.
37. Peña, V.; Barbara, I. Seasonal patterns in the mäerl community of shallow European Atlantic beds and their use as a baseline for monitoring studies. *Eur. J. Phycol.* **2010**, *45*, 327–342.
38. Pardo, C.; Lopez, L.; Peña, V.; Hernández-Kantún, J.; Le Gall, L.; Bárbara, I.; Barreiro, R. A multilocus species delimitation reveals a striking number of species of coralline algae forming maërl in the OSPAR Maritime Area. *PLoS ONE* **2014**, *9*, e104073.
39. Thrush, S.F.; Schneider, D.C.; Legendre, P.; Whitlatch, R.B.; Dayton, P.K.; Hewitt, J.E.; Hines, A.H.; Cummings, V.J.; Lawrie, S.M.; Grantet, J.; et al. Scaling-up from experiments to complex ecological systems: Where to next? *J. Exp. Mar. Biol. Ecol.* **1997**, *216*, 243–254.
40. Wootton, J.T. Local interactions predict large-scale pattern in empirically derived cellular automata. *Nature* **2001**, *413*, 841–843.
41. Irving, A.D.; Connell, S.D.; Gillanders, B.M. Local complexity in patterns of canopy-benthos associations produces regional patterns across temperate Australasia. *Mar. Biol.* **2004**, *144*, 361–368.
42. Fraschetti, S.; Bianchi, C.N.; Terlizzi, A.; Fanelli, G.; Morri, C.; Boero, F. Spatial variability and human disturbance in shallow subtidal hard substrate assemblages: A regional approach. *Mar. Ecol. Prog. Ser.* **2001**, *212*, 1–12.
43. Fraschetti, S.; Terlizzi, A.; Benedetti-Cecchi, L. Patterns of distribution of marine assemblages from rocky shores: Evidence of relevant scales of variation. *Mar. Ecol. Prog. Ser.* **2005**, *296*, 13–29.
44. Steneck, R.S. The ecology of coralline algal crusts: Convergent patterns and adaptive strategies. *Ann. Rev. Ecol. Syst.* **1986**, *17*, 273–303.
45. Lanfranco, E.; Rizzo, M.; Hall-Spencer, J.; Borg, J.A.; Schembri, P.J. Maerl-forming coralline algae and associated phytobenthos from the Maltese Islands. *Cent. Mediterr. Nat.* **1999**, *3*, 1–6.
46. Ballesteros, E. Mediterranean coralligenous assemblages: A synthesis of present knowledge. *Oceanogr. Mar. Biol.* **2006**, *44*, 123–195.
47. Chimienti, G.; Stithou, M.; Dalle Mura, I.; Mastrototaro, F.; D'Onghia, G.; Tursi, A.; Izzi, C.; Fraschetti, S. An explorative assessment of the importance of mediterranean coralligenous habitat to local economy: The case of recreational diving. *J. Environ. Account. Manag.* **2017**, *5*, 315–325.
48. Piazzi, L.; Kaleb, S.; Ceccherelli, G.; Montefalcone, M.; Falace, A. Deep coralligenous outcrops of the Apulian continental shelf: Biodiversity and spatial variability of sediment-regulated assemblages. *Cont. Shelf. Res.* **2019**, *172*, 50–56.
49. Pérès, J.M.; Picard, J. Nouveau manuel de bionomie benthique de la Mer Méditerranée. *Rec. Travl St. Mar. Endoume* **1964**, *31*, 5–137.
50. Bedulli, D.; Bianchi, C.N.; Zurlini, G.; Morri, C. Caratterizzazione biocenotica e strutturale del macrobenthos delle coste pugliesi. In *Indagine Ambientale del Sistema Marino Costiero della Regione Puglia*; Viel, M., Zurlini, G., Eds.; ENEA: Rome, Italy, 1986; pp. 227–255.
51. Damiani, V.; Bianchi, C.N.; Ferretti, O.; Bedulli, D.; Morri, C.; Viel, M.; Zurlini, G. Risultati di una ricerca ecologica sul sistema marino costiero pugliese. *Thalassia Salentina* **1988**, *18*, 153–169.
52. Matarrese, A.; Panza, M.; Mastrototaro, F.; Costantino, G. Preliminare rappresentazione cartografica dei fondali dell'arcipelago delle Isole Tremiti (Mar Adriatico). *Biol. Mar. Mediterr.* **2000**, *7*, 590–593.
53. Tropeano, M.; Spalluto, L. Present-day temperate-type carbonate sedimentation on Apulia shelves (southern Italy). *GeoActa* **2006**, *5*, 129–142.
54. Martin, C.; Giannoulaki, M.; De Leo, F.; Scardi, M.; Salomidi, M.; Knittweis, L.; Pace, M.L.; Garofalo, G.; Gristina, M.; Ballesteros, E. Coralligenous and maërl habitats: Predictive modelling to identify their spatial distributions across the Mediterranean Sea. *Sci. Rep.* **2015**, *4*, 5073.

55. Cushman-Roisin, B.; Gacic, M.; Poulain, P.M.; Artegiani, A. *Physical Oceanography of the Adriatic Sea: Past, Present and Future*; Springer: Dordrecht, The Netherlands, 2001; pp. 1–304.
56. Millot, C.; Taupier-Letage, I. Circulation in the Mediterranean Sea. In *The Mediterranean Sea. Handbook of Environmental Chemistry*; Sailot, A., Ed.; Springer: Berlin/Heidelberg, Germany, 2005; Volume 5K, pp. 29–66.
57. Chimienti, G.; De Padova, D.; Mossa, M.; Mastrototaro, F. A mesophotic black coral forest in the Adriatic Sea. *Sci. Rep.* **2020**, *10*, 1–15.
58. Aiello, G.; Budillon, F. Lowstand prograding wedges as fourth-order glacio-eustatic cycles in the Pleistocene continental shelf of Apulia (southern Italy). In *Cyclostratigraphy: Approaches and Case Histories*; D'Argenio, B., Fisher, A.G., Premoli Silva, I., Weissert, H., Ferreri, V., Eds.; Society for Sedimentary Geology: Tusla, OK, USA, 2014; pp. 215–230.
59. Senatore, M.R. Terrazzi deposizionali sommersi lungo il margine ionico della Puglia. *Mem. Descr. Carta Geol. d'It.* **2004**, *58*, 141–146.
60. Poulain, P.M. Adriatic Sea surface circulation as derived from drifter data between 1990 and 1999. *J. Mar. Syst.* **2001**, *29*, 3–32.
61. Artale, V.; Zoccolotti, L. Alcuni aspetti della circolazione dell'Adriatico e formazione di acque dense. In *Indagine Ambientale del Sistema Marino Costiero della Regione Puglia*; Viel, M., Zurlini, G., Eds.; ENEA: Rome, Italy, 1986; pp. 87–99.
62. Mosetti, F. Caratteristiche fondamentali dell'idrologia dell'Adriatico. *Boll. Ocean. Teor. Appl.* **1984**, *2*, 169–194.
63. Artegiani, A.; Paschini, E.; Russo, A.; Bregnt, D.; Raicich, F.; Pinardi, N. The Adriatic Sea general circulation. Part II: Baroclinic circulation structure. *J. Phys. Oceanogr.* **1997**, *27*, 1515–1532.
64. Cattaneo, A.; Correggiari, A.; Langone, L.; Trincardi, F. The late-Holocene Gargano subaqueous delta, Adriatic shelf: Sediment pathways and supply fluctuations. *Mar. Geol.* **2003**, *193*, 61–91.
65. Caldara, M.; Centenaro, E.; Mastronuzzi, G.; Sansò, P.; Sergio, A. Features and present evolution of Apulian coast (Southern Italy). *J. Coast. Res.* **1998**, *SI26*, 55–64.
66. Gasparini, G.P.; Griffa, A.L. Studio delle condizioni dinamiche nel Golfo di Taranto. In *Indagine Ambientale del Sistema Marino Costiero della Regione Puglia*; Viel, M., Zurlini, G., Eds.; ENEA: Rome, Italy, 1986; pp. 101–125.
67. Savini, A.; Basso, D.; Bracchi, V.A.; Corselli, C.; Pennetta, M. Maerl-bed mapping and carbonate quantification on submerged terraces offshore the Cilento peninsula (Tyrrhenian Sea, Italy). *Geodiversitas* **2012**, *34*, 77–98.
68. Chimienti, G.; Angeletti, L.; Rizzo, L.; Tursi, A.; Mastrototaro, F. ROV vs trawling approaches in the study of benthic communities: The case of *Pennatula rubra* (Cnidaria: Pennatulacea). *J. Mar. Biol. Assoc.* **2018**, *98*, 1859–1869.
69. Weinberg, S. The minimal area problem in invertebrate communities of Mediterranean rocky substrata. *Mar. Biol.* **1978**, *49*, 33–40.
70. Chimienti, G. Vulnerable forests of the pink sea fan *Eunicella verrucosa* in the Mediterranean Sea. *Diversity* **2020**, *12*, 176.
71. Kaleb, S.; Alongi, G.; Falace, A. Coralline algae preparation for scanning electron microscopy and optical microscopy. In *Protocols for Macroalgae Research*; Charrier, B.; Wichard, T.; Reddy, C.R.K., Ed.; Taylor and Franciss Group: Boca Raton, FL, USA, 2018; pp. 413–429.
72. Guiry, M.D.; Guiry, G.M. AlgaeBase. *World-Wide Electronic Publication*; National University of Ireland: Galway, Ireland, 2020. Available online: http://www.algaebase.org (accessed on 20 July 2020).
73. Clarke, K.R.; Gorley, R.H. *PRIMER V6: User Manual/Tutorial*; Primer-e: Plymouth, UK, 2001.
74. Anderson, M. A new method for non-parametric multivariate analysis of variance. *Austral. Ecol.* **2001**, *26*, 32–46.
75. Anderson, M.J.; ter Braak, C.J.F. Permutation tests for multi-factorial analysis of variance and regression. *J. Stat. Comput. Simul.* **2003**, *73*, 85–113.
76. Anderson, M.J.; Diebel, C.E.; Blom, W.M.; Landers, T.J. Consistency and variation in kelp holdfast assemblages: Spatial patterns of biodiversity for the major phyla at different taxonomic resolutions. *J. Exp. Mar. Biol. Ecol.* **2005**, *320*, 35–56.
77. Anderson, M.J. Distance-based tests for homogeneity of multivariate dispersion. *Biometrics* **2006**, *62*, 245–253.

78. Anderson, M.J.; Ellingsen, K.E.; McArdle, B.H. Multivariate dispersion as a measure of beta diversity. *Ecol. Lett.* **2006**, *9*, 683–693.
79. Clarke, K.R. Non-parametric multivariate analyses of changes in community structure. *Aust. J. Ecol.* **1993**, *18*, 117–143.
80. Lambshead, P.J.D.; Piatt, H.M.; Shaw, K.M. The detection of differences among assemblages of marine benthic species based on an assessment of dominance and diversity. *J. Nat. Hist.* **1983**, *17*, 859–974.
81. Rocha, G.A.; Bastos, A.C.; Amado-Filho, G.M.; Boni, G.C.; Moura, R.L.; Oliveira, N. Heterogeneity of rhodolith beds expressed in backscatter data. *Mar. Geol.* **2020**, *423*, 106136.
82. Le Bas, T.P.; Huvenne, V.A.I. Acquisition and processing of backscatter data for habitat mapping—Comparison of multibeam and sidescan systems. *Appl. Acoust.* **2009**, *70*, 1248–1257.
83. Otero-Ferrer, F.; Cosme, M.; Tuya, F.; Espino, F.; Haroun, R. Effect of depth and seasonality on the functioning of rhodolith seabeds. *Estuar. Coast. Shelf. Sci.* **2020**, *235*, 106579.
84. Thrush, S.F.; Pridmore, R.D.; Hewitt, J.E. Impacts on soft-sediment macrofauna: The effects of spatial variation on temporal trends. *Ecol. Appl.* **1994**, *4*, 31–41.
85. Coleman, R.A.; Browne, M.; Theobalds, T. Small-scale spatial variability in intertidal and subtidal turfing algal assemblages and the temporal generality of these patterns. *J. Exp. Mar. Biol. Ecol.* **2002**, *267*, 53–74.
86. Schubert, N.; Salazar, V.W.; Rich, W.A.; Bercovich, M.V.; Saá, A.A.; Fadigas, S.D.; Silva, J.; Horta, P.A. Rhodolith primary and carbonate production in a changing ocean: The interplay of warming and nutrients. *Sci. Total Environ.* **2019**, *676*, 455–468.
87. Carvalho, V.F.; Assis, J.; Serrão, E.A.; Nunes, J.M.; Anderson, A.B.; Batista, M.B.; Barufi, J.B.; Silva, J.; Pereira, S.M.B.; Horta, P.A. Environmental drivers of rhodolith beds and epiphytes community along the South Western Atlantic coast. *Mar. Environ. Res.* **2020**, *154*, 104827.
88. Agnesi, S.; Annunziatellis, A.; Inghilesi, R.; Orasi, A. The contribution of wind-wave energy at sea bottom to the modelling of rhodolith beds distribution in an off-shore continental shelf. *Mediterr. Mar. Sci.* **2020**, *21*, 433–441.
89. Bosellini, A.; Ginsburg, R. Form and internal structure of recent algal nodules (Rhodolites) from Bermuda. *J. Geol.* **1971**, *79*, 669–682.
90. Crocetta, F.; Riginella, E.; Lezzi, M.; Tanduo, V.; Balestrieri, L.; Rizzo, L. Bottom-trawl catch composition in a highly polluted coastal area reveals multifaceted native biodiversity and complex communities of fouling organisms on litter discharge. *Mar. Environ. Res.* **2020**, *155*, 104875.
91. Rendina, F.; Ferrigno, F.; Appolloni, L.; Donnarumma, L.; Sandulli, R.; Fulvio, G. Anthropic pressure due to lost fishing gears and marine litter on different rhodolith beds off the Campania Coast (Tyrrhenian Sea, Italy). *Ecol. Quest.* **2020**, *31*, 1–17.
92. Barberá, C.; Mallol, S.; Vergés, A.; Cabanellas-Reboredo, M.; Díaz, D.; Goñi, R. Maerl beds inside and outside a 25-year-old no-take area. *Mar. Ecol. Prog. Ser.* **2017**, *572*, 77–90.
93. Gennaro, P.; Piazzi, L. Synergism between two anthropic impacts: *Caulerpa racemosa* var. *cylindracea* invasion and seawater nutrient enrichment. *Mar. Ecol. Prog. Ser.* **2011**, *427*, 59–70.
94. Klein, J.; Verlaque, M. The *Caulerpa racemosa* invasion: A critical review. *Mar. Pollut. Bull.* **2008**, *56*, 205–225.
95. Piazzi, L.; Balata, D.; Bulleri, F.; Gennaro, P.; Ceccherelli, G. The invasion of *Caulerpa cylindracea* in the Mediterranean: The known, the unknown and the knowable. *Mar. Biol.* **2016**, *163*, 161.
96. Rizzo, L.; Pusceddu, A.; Bianchelli, S.; Fraschetti, S. Potentially combined effect of the invasive seaweed *Caulerpa cylindracea* (Sonder) and sediment deposition rates on organic matter and meiofaunal assemblages. *Mar. Environ. Res.* **2020**, *159*, 104966.
97. Rizzo, L.; Pusceddu, A.; Stabili, L.; Alifano, P.; Fraschetti, S. Potential effects of an invasive seaweed (*Caulerpa cylindracea*, Sonder) on sedimentary organic matter and microbial metabolic activities. *Sci. Rep.* **2017**, *7*, 12113.
98. Martin, S.; Gattuso, J.P. Response of Mediterranean coralline algae to ocean acidification and elevated temperature. *Glob. Chang. Biol.* **2009**, *15*, 2089–2100.
99. McCoy, S.J.; Ragazzola, F. Skeletal trade-offs in coralline algae in response to ocean acidification. *Nat. Clim. Chang.* **2014**, *4*, 719–723.
100. Rindi, F.; Braga, J.; Martin, S.; Peña, V.; Le Gall, L.; Caragnano, A.; Aguirre, J. Coralline algae in a changing Mediterranean Sea: How can we predict their future, if we do not know their present? *Front. Mar. Sci.* **2019**, *6*, 723.

101. Martin, S.; Cohu, S.; Vignot, C.; Zimmerman, G.; Gattuso, J.P. One-year experiment on the physiological response of the Mediterranean crustose coralline alga, *Lithophyllum cabiochae*, to elevated pCO_2 and temperature. *Ecol. Evol.* **2013**, *3*, 676–693.
102. Vásquez-Elizondo, R.M.; Enríquez, S. Coralline algal physiology is more adversely affected by elevated temperature than reduced pH. *Sci. Rep.* **2016**, *6*, 19030.
103. Martin, S.; Hall-Spencer, J.M. Effects of ocean warming and acidification on rhodolith/maërl beds. In *Rhodolith/Maërl Beds: A Global Perspective*; Riosmena-Rodríguez, R., Nelson, W., Aguirre, J., Eds.; Springer International Publishing: Cham, Switzerland, 2018; pp. 55–85.
104. Chimienti, G.; Bo, M.; Taviani, M.; Mastrototaro, F. Occurrence and Biogeography of Mediterranean Cold-Water Corals. In *Mediterranean Cold-Water Corals: Past, Present and Future*; Orejas, C., Jimennez, C., Eds.; Springer International Publishing: Berlin, Germany, 2019; Volume 9, pp. 213–243.
105. Morato, T.; González-Irusta, J.M.; Dominguez-Carrió, C.; Wei, C.L.; Davies, A.; Sweetman, A.K.; Taranto, G.H.; Beazley, L.; García-Alegre, A.; Grehan, A.; et al. Climate-induced changes in the suitable habitat of cold-water corals and commercially important deep-sea fishes in the North Atlantic. *Glob. Chang. Biol.* **2020**, *26*, 2181–2202.